Functional Colocalization of Water Channels and Proton Pumps in Endosomes from Kidney Proximal Tubule

RENGAO YE, LAN-BO SHI, WAYNE I. LENCER, and A. S. VERKMAN

From the Department of Medicine, Cardiovascular Research Institute, University of California, San Francisco, California 94143; and the Renal Unit, Massachusetts General Hospital, Boston, Massachusetts 02114

ABSTRACT The apical membrane of mammalian proximal tubule undergoes rapid membrane cycling by exocytosis and endocytosis. Osmotic water and ATP-driven proton transport were measured in endocytic vesicles from rabbit and rat proximal tubule apical membrane labeled in vivo with the fluid phase marker fluorescein-dextran. Osmotic water permeability (P_f) was determined from the time course of fluorescein-dextran fluorescence after exposure of endosomes to an inward osmotic gradient in a stopped-flow apparatus. P_f was 0.009 (rabbit) and 0.029 cm/s (rat) (23°C) and independent of osmotic gradient size. P_f in rabbit endosomes was inhibited reversibly by $HgCl_2$ (K_I = 0.2 mM) and had an activation energy of 6.4 ± 0.5 kcal/mol (15–35°C). Endosomal proton ATPase activity was measured from the time course of internal pH, measured by fluorescein-dextran fluorescence, after the addition of external ATP. Endosomes contained an ATP-driven proton pump that was sensitive to *N*-ethylmaleimide and insensitive to vanadate and oligomycin. In response to saturating [ATP] the pump acidified the endosomal compartment at a rate of 0.17 (rat) and 0.029 pH unit/s (rabbit); at an external pH of 7.4, the steady-state pH was 6.4 (rat) and 6.5 (rabbit). To examine whether water channels and the proton ATPase were present in the same endosome, the time course of fluorescein-dextran fluorescence was measured in response to an osmotic gradient in the presence and absence of ATP. ATP did not alter endosome P_f, but decreased the amplitude of the fluorescence signal by 43 ± 3% (rabbit) and 47 ± 4% (rat). The signal decrease was reversed by nigericin, which collapsed the ATP-dependent pH gradient, indicating that the water channel and proton ATPase were localized to the same endosome. In addition, there was no evidence for the presence of a sodium/proton exchanger or a sodium/glucose cotransporter in these endosomes even though both proteins are known to be present in the apical membrane of proximal tubule cells. These findings demonstrate the selective retrieval of water channels and proton pumps from the apical membrane of mammalian proximal tubule epithelia into an endosomal compartment capable of maintaining an acidic pH.

Address reprint requests to Dr. Alan S. Verkman, 1065 Health Sciences East Tower, Cardiovascular Research Institute, University of California, San Francisco, CA 94143.

J. GEN. PHYSIOL. © The Rockefeller University Press · 0022-1295/89/05/0885/18 $2.00
Volume 93 May 1989 885–902

INTRODUCTION

The kidney proximal tubule resorbs the majority of water, bicarbonate, sodium, and glucose filtered by the glomerulus. The apical membrane of the proximal tubule epithelium has been shown to contain a number of transporters dedicated to fluid and solute resorption including water channels (Whittembury et al., 1985; van Heeswijk and van Os, 1986; Meyer and Verkman, 1987), sodium-proton exchange (Warnock et al., 1982), sodium-glucose cotransport (Hopfer and Groseclose, 1980; Fromter, 1984) and likely, a proton ATPase (Preisig et al., 1987; Sabolic and Burckhardt, 1988). In addition, the proximal tubule apical membrane undergoes very rapid turnover by exocytosis and endocytosis of intracellular vesicles (Strauss, 1964; Bode et al., 1974; Rodman et al., 1986); endocytic vesicles from proximal tubule have been shown to contain a proton ATPase (Sabolic et al., 1985) and there is controversy about whether these vesicles contain a sodium-proton exchanger (Sabolic et al., 1985; Gurich and Warnock, 1986).

Whereas the exocytic-endocytic cycle in amphibian epithelia and principal cells of the kidney collecting tubule is thought to regulate apical membrane water permeability (Wade et al., 1981; Verkman et al., 1988; Shi and Verkman, 1989), the role of the rapid membrane cycling in the proximal tubule is totally unknown. Recent studies suggest that apical membrane endocytosis is, in part, under direct control by hormones and effectors of calcium and protein kinase C pathways (O'Neil and Reid, 1988; Park, 1988). It has been suggested that apical membrane cycling in the proximal tubule may be important for regulation of water transport (Berry and Verkman, 1988) and bicarbonate resorption (Gurich and Warnock, 1986), and for the insertion and retrieval of specific membrane transporters, such as the sodium-proton exchanger and the sodium-glucose cotransporter, in response to metabolic need. If so, these membrane transport proteins should be present and functional in endocytic vesicles.

We report here an analysis of the water and proton transport pathways in endocytic vesicles from the rabbit and rat proximal tubule. Endocytic vesicles were labeled selectively in the in vivo kidney by intravenous infusion of a fluorescein-labeled dextran as we reported recently for analysis of vasopressin-sensitive water transport in the kidney collecting tubule (Verkman et al., 1988). Osmotic water transport, sodium and ATP-driven proton transport, and sodium-dependent D-glucose transport were examined in isolated endosomes by making use of the sensitivity of fluorescein-dextran fluorescence to endosomal pH and volume. We found that proximal tubule endosomes contain a mercurial-inhibitable water channel with low activation energy similar to that found in the proximal tubule apical membrane, and an oligomycin-resistant, *N*-ethylmaleimide (NEM)-sensitive proton ATPase. Individual endosomes contained both water channels and proton pumps. In contrast, endosomes did not have measurable sodium-proton exchange or sodium-glucose cotransport activity, demonstrating selective retrieval of apical membrane transporters.

METHODS

Materials

Fluorescein-dextran (10,000 D) and ATP were obtained from Sigma Chemical Co. (St. Louis, MO). Fluorescein-dextran was dialyzed overnight to remove unconjugated fluorescein.

ATP solutions were prepared within 4 h of use. The inhibitors oligomycin, vanadate, and NEM were obtained from Aldrich Chemical Co. (Milwaukee, WI). The ionophores valinomycin and nigericin were obtained from Sigma Chemical Co. and were stored as 5 mg/ml stock solutions in ethanol.

Endosome Isolation

Female New Zealand white rabbits (1.5–2 kg) were anesthetized with sodium pentobarbital (30 mg/kg i.v.). Fluorescein dextran (10,000 D, 500 mg in 10 ml of phosphate-buffered saline, PBS) was infused over 1 min. i.v. Unless stated otherwise, after an additional 10–12 min, kidneys were perfused in vivo through the renal artery with ~30 ml of cold PBS while the aorta was clamped proximally. Subsequent steps were carried out at 4°C. Kidneys were removed and cortical slices (0.5–1 mm deep) were dissected and placed in homogenizing buffer (100 mM KCl, 5 mM K phosphate, 2 mM $MgCl_2$, pH 7.4/ or 100 mM mannitol, 5 mM K phosphate, pH 7.4). The cortex was homogenized by 15 strokes of a Potter-Elvehjem homogenizer. To remove tissue debris and mitochondria, the sample was centrifuged for 10 min at 750 *g*; the supernatant was centrifuged for an additional 10 min at 5,000 *g*. The resultant supernatant was spun at 100,000 *g* for 1 h to obtain the crude microsomal pellet, which contained proximal tubule endosomes labeled with fluorescein-dextran. The pellet was washed once in > 50 vol of homogenizing buffer, and then suspended at a concentration of ~5 mg/ml and homogenized using 22 and 27 gauge steel needles. Cortical endosomes from Brattleboro rats were isolated by a similar procedure as described previously (Verkman et al., 1988). Experiments were performed immediately after microsome preparation.

Morphological Characterization of Endosomes

To determine endosome size, animals were infused intravenously with horseradish peroxidase (HRP; ~100 mg/kg) in place of fluorescein-dextran. The microsomal fraction prepared as above was fixed in 2% gluteraldehyde, reacted with diaminobenzidine and H_2O_2, and visualized by thin section electron microscopy (~70 nm sections) as described previously (Verkman et al., 1988). Endosomes for both rabbit and rat had a unimodal Gaussian distribution in endosome diameter with a mean of 135 ± 30 nm, similar to the size of HRP-labeled endosomes in rat kidney sections reported by Sabolic et al. (1985). 2–5% of vesicles in the microsomal pellet contained HRP. To show that the majority of endosomes labeled with fluorescein-dextran were derived from the apical surface of proximal tubule, kidneys were fixed in vivo and semithin cryosections were examined by fluorescence microscopy using a new fixation method that preserves the intracellular geometry (Weyer et al., 1988). It was reported that > 95% of fluorescence in cortical slices came from subapical endosomes of proximal tubule cells. These results are in agreement with studies of HRP localization in rats injected with HRP 15 min before kidney removal (Rodman et al., 1986). Because of the small number of cortical collecting tubules in the superficial cortex and because of the relatively low levels of endocytosis in collecting tubules compared with proximal tubules, there was little contamination of the microsomal fraction by fluorescein-dextran–labeled endosomes from collecting tubule.

Osmotic Water Transport Measurements

Osmotic water permeability was measured by a stopped-flow fluorescence technique as described by Chen et al. (1988). 75 μl of a microsome suspension (~0.1 mg/ml) containing endosomes labeled with fluorescein-dextran were subject to specified inward sucrose gradients using a Hi-Tech SF-51 stopped-flow apparatus (Wiltshire, England). The instrument dead time was under 2 ms. Temperature was controlled by a circulating water bath and monitored by an indwelling thermistor. Fluorescence was excited by a stabilized tungsten-halogen

lamp and a single grating monochromator (480 ± 5 nm) in series with a six-cavity broad band (420–490 nm) interference filter. Fluorescence was monitored through two OG515 cut-on filters in series (Schott Glass, Duryea, PA). Data were recorded at a maximum rate of 10 points/ms and stored on a MINC/23 computer (Digital Equipment Corp., Marlboro, MA) for analysis. 512 time points were acquired in each experiment. Generally, each measurement of water permeability was repeated 10 times for signal averaging. Data were fitted to single (rabbit) or double (rat) exponential functions (see Results). Osmotic water permeability coefficients (P_f) were calculated by comparing exponential time constants of experimental data with exponential time constants of theoretical curves calculated from the Kedem-Katchalsky equations in which P_f was varied (Chen et al., 1988).

In some experiments, ATP (5 mM) was added to the microsome suspension from a 100-mM stock solution titrated to pH 7.40. Stopped-flow experiments were carried out before and 3–5 min after addition of ATP using the same microsome suspension without changing the instrument gain settings. Additional stopped-flow experiments were carried out after addition of nigericin (~5 μM, 6.8 mM ethanolic stock) to the endosome suspension to equilibrate endosome and solution pH.

Proton Pump Activity Measurements

Passive, Na gradient-driven, and ATP-driven proton permeabilities were measured in endosomes labeled with fluorescein-dextran. Microsomes (final concentration, ~20 μg protein/ml) were added to 2 ml of buffer containing 100 mM KCl, 2 mM $MgCl_2$, and 5 mM K phosphate at pH 7.40 in an acrylic cuvette in a temperature-jacketed chamber. The solution was stirred continuously. Fluorescence was measured using an SLM Instruments 48000 fluorometer (Urbana, IL) interfaced to an IBM PC/AT computer at an excitation wavelength of 480 ± 4 and an emission of > 515 nm. Data were averaged over 1-s time intervals.

For measurement of passive and ATP-driven proton transport, valinomycin (4.5 μM, 4.5 mM ethanolic stock) was added to the stirred microsome suspension to eliminate diffusion potentials. Further increases in the valinomycin concentration caused no further increase in proton transport rates, demonstrating the adequacy of the voltage clamp. ATP was added from a 100-mM stock solution. After endosome pH stabilized, nigericin (~5 μM) was added to collapse the pH gradient. To determine the relationship between measured fluorescence intensity and absolute endosomal pH, it was necessary to correct the fluorescence signal for the fluorescence arising from external fluorescein-dextran. In every experiment, aliquots of a polyclonal anti-fluorescein antibody raised in rabbits were added to quench the external fluorescence signal (see Results). To determine the baseline signal at the end of each experiment, 100 μl of 1 M HCl was added to quench the fluorescence signal completely. The baseline signal was always < 5% of the total signal. The total fluorescence signal was corrected for the contribution from external fluorescein-dextran fluorescence and the baseline fluorescence. A second independent method was used to determine the internal fluorescence signal that relied on analysis of the amplitudes of the rapid and slow fluorescence decrease after addition of HCl to drop the pH to 6.5 (Verkman and Ives, 1986). Results from the two methods were in quantitative agreement.

Sodium-Proton Exchange Measurement

Passive (Na and ATP-independent) proton permeability was measured from the time course of fluorescence following serial additions of HCl and KOH (containing NaCl or choline Cl) to the voltage-clamped microsome suspension. Endosomes containing 100 mM KCl, 2 mM $MgCl_2$, and 5 mM K phosphate at pH 7.4, and voltage-clamped with valinomycin were suspended in the same buffer. HCl was added from a 1-M stock solution in H_2O to drop solution pH to 6.5, which resulted in proton influx until endosome pH reached 6.5. To determine

whether the endosomes contained a sodium-proton exchanger, an aliquot of 1 M KOH containing NaCl or choline chloride was then added to return external pH to 7.4. Final external NaCl or choline Cl concentration was 20 mM. The initial rate of endosome alkalinization was determined (internal pH 6.5, external pH 7.4) from the initial rate of fluorescence increase. Presence of a sodium-proton exchanger would result in an enhanced rate of alkalinization after the addition of KOH containing NaCl compared with the addition of KOH containing choline Cl. The small increase in external osmolarity after NaCl or choline Cl addition (internal osmolarity 215 mosmol, external osmolarity 245 mosmol) resulted in an immediate (< 0.25 s) decrease in vesicle volume by ~19%, causing a ~2% decrease in fluorescence (determined as in Fig. 1 *B* using the 100 mM KCl buffer); this theoretical small fluorescence decrease was not observable and would not alter the interpretation of data.

Nonelectrolyte and Sodium/Glucose Transport Measurements

The permeability of endosomes to a series of small polar nonelectrolytes (urea, ethylene glycol, and glycerol) was measured by stopped-flow fluorescence. Endosomes were subject to a 100-mM inward gradient of each solute. Nonelectrolyte permeability coefficients (P_s) were calculated from the time course of endosome fluorescence during the phase of nonelectrolyte influx, after the initial water efflux had occurred (see Results) (Chen et al., 1988).

The presence of sodium-dependent D-glucose transport was examined in endosomes by measurement of volume changes accompanying D-glucose uptake as reported recently (Kim et al., 1988). Labeled, voltage-clamped microsomes, in a buffer containing 25 mM KCl, and 5 mM K phosphate at pH 7.4, were subject to a 100 mM inward D-glucose gradient in the presence and absence of 100 μM phloretin. The entry of 1 mol of glucose via a sodium-glucose cotransporter would effect the entry of 1 mol of sodium and the exit of 1 mol of potassium, which would result in the net entry of 1 osmol of solute, causing endosome swelling.

RESULTS

Osmotic Water Permeability

The osmotic water permeability of endosomes labeled with fluorescein-dextran was determined from the time course of fluorescence self-quenching in response to inward osmotic gradients of sucrose (Fig. 1). An inward osmotic gradient caused water efflux and a decrease in endosome volume resulting in a time-dependent decrease in fluorescence intensity. There was no change in fluorescence in the absence of an osmotic gradient (top trace), indicating the absence of mixing artifacts in the stopped-flow apparatus. With increasing osmotic gradient size, the signal amplitude and rate of fluorescence drop increased as predicted by equations describing the time course of vesicle volume in response to an osmotic gradient (Verkman et al., 1985). For the smaller osmotic gradients (25–200 mosmol) data for rabbit endosomes fitted closely to a single exponential function, indicating functionally the presence of a single class of endosomes with respect to water transport. As given below, the time course of fluorescence in rat endosomes required a biexponential fit, indicating the presence of two functional classes of endosomes with respect to water transport.

To examine whether endosome water transport occurred by a specialized channel or pore mechanism rather than by passive diffusion through membrane phospholipid, the absolute osmotic water permeability coefficient (P_f), the activation energy

(E_a) and the effects of water transport inhibitors were determined. It has been established empirically in erythrocytes and renal tissues that the presence of a water channel is associated with a high P_f (> 0.005 cm/s at 23°C), low E_a (~5 kcal/mol), and inhibition by mercurials (Macey, 1984; Finkelstein, 1987; Meyer and Verkman, 1987). In contrast, water movement via a phospholipid pathway is generally associated with low P_f (< 0.005 cm/s), high E_a (10–20 kcal/mol), and lack of effect of mercurial inhibitors on water transport.

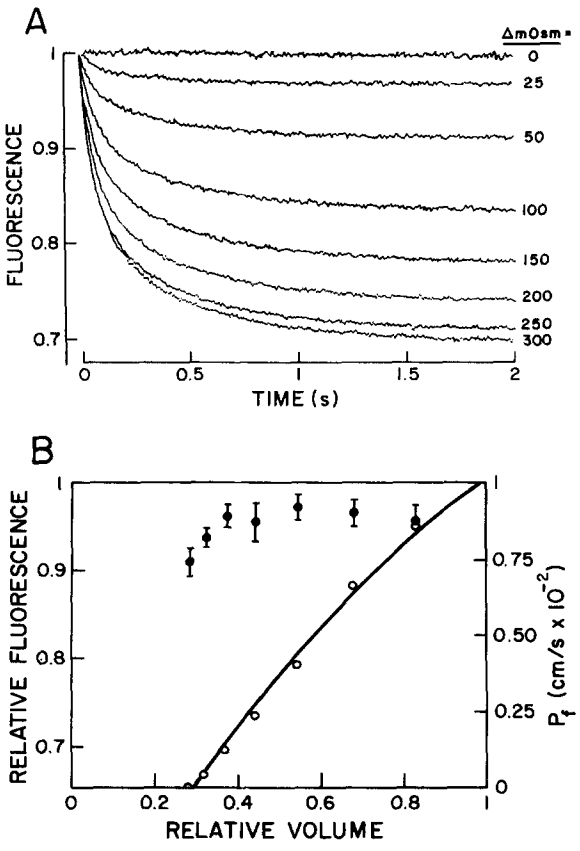

FIGURE 1. Osmotic gradient dependence of water transport in rabbit endosomes. Endosomes containing 100 mM mannitol, 5 mM K phosphate, and fluorescein-dextran at pH 7.4 were subject to inward sucrose gradients in a stopped-flow apparatus as described in Methods. (*A*) The time course of fluorescence normalized to unity at zero time is given. The magnitude of the inward sucrose gradient is given to the right of each curve. (*B*) Fluorescence, determined from a single exponential fit of the time course data extrapolated to infinite time, is plotted against relative endosome volume, determined from the ratio of internal to external osmolarities after mixing (open circles). Data were fitted to the empiric quadratic relation, fluorescence = $-0.210\ V^2 + 0.693\ V + 0.517$, where V is relative volume. P_f values (closed squares) corresponding to data at each osmotic gradient were calculated as described in Methods using an endosome surface-to-volume ratio of 4.4×10^5 cm^{-1}.

To determine endosome P_f from the fluorescence kinetic data, an empiric relationship between endosome fluorescence and volume must be established. It is not correct to assume that the self-quenching properties of fluorescein-dextran are the same in free solution as when entrapped in membrane vesicles (Chen et al., 1988); the presence of membrane proteins greatly enhances the apparent self-quenching characteristics of fluorescein compounds. Fig. 1, (bottom) shows the dependence of endosome fluorescence (inferred from the amplitude of single exponentials fitted to

the time course) on relative endosome volume (calculated from the ratio of initial to final endosome osmolalities). Data were slightly curvilinear over the range of volumes used experimentally. P_f in centimeters per second was calculated from the fluorescence time course, fluorescence vs. volume calibration, and endosome surface-to-volume ratio as described in Methods. Calculated P_f (0.008–0.009 cm/s) was independent of osmotic gradient size for inward gradients of under 200 mosmol.

The effect of $HgCl_2$ on osmotic water transport in rabbit endosomes is shown in Fig. 2. There was a dose-dependent, marked inhibition of water transport, with 74 ± 3% (SD, $n = 6$) decrease in P_f at 1 mM $HgCl_2$, and 50% inhibition of P_f at 0.32 ± 0.03 mM $HgCl_2$, based on the fit of data to a single-site saturable binding model. It is notable that only a single functional population of endosomes was present at all [$HgCl_2$] which suggests that water transport in all labeled endosomes was inhibit-

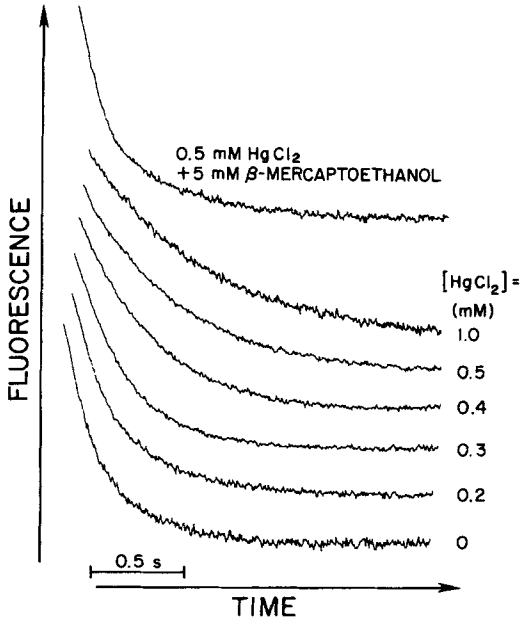

FIGURE 2. Inhibition of endosome water transport by $HgCl_2$. Experiments were performed as described in the legend to Fig. 1 using a 100-mM inward sucrose gradient. $HgCl_2$ was added to the endosome suspension 5 min before measurements. Mercaptoethanol was added to the suspension containing 0.5 mM $HgCl_2$ and incubated for 1 min. Curves were displaced for visual clarity.

able. Inhibition of transport by 0.5 mM $HgCl_2$ was reversed > 95% ($n = 6$) with addition of 5 mM mercaptoethanol. Mercaptoethanol itself did not alter P_f in the absence of $HgCl_2$. The compounds NEM (1 mM), phloretin (0.25 mM), and H_2DIDS (0.5 mM) did not inhibit osmotic water transport.

The temperature dependence for P_f measured in the presence and absence of 0.5 mM $HgCl_2$ is given in Table I. In the absence of inhibitor, P_f approximately doubled over a 15–35°C temperature range, corresponding to an E_a of 6.4 ± 0.5 kcal/mol based on a linear regression to an Arrhenius plot of the data. The inhibitory potency of $HgCl_2$ decreased with increasing temperature, which is consistent with a higher E_a for the noninhibitable, lipid pathway for water, than for the inhibitable pathway.

Similar results were obtained using endosomes from the renal cortex of Brattleboro rats. In six independent sets of measurements on rat endosomes subject to a

100 mosmol inward sucrose gradient, fitted exponential time constants for the fluorescence time course were 42 ± 4 and 640 ± 30 ms, corresponding to P_f values of 0.029 and 0.002 cm/s, respectively. The fractional signal amplitude for the faster component of water transport was 0.64 ± 0.03. The fast component of water transport was inhibited reversibly by $HgCl_2$ with 50% inhibition at ~0.3 mM $HgCl_2$; there was little effect of $HgCl_2$ on the slower component of water transport. Based on two sets of temperature dependence studies, E_a for the faster and slower components of water transport was 3.2 ± 0.5 and 9.6 ± 0.8 kcal/mol, respectively. Though more difficult to interpret because of functional heterogeneity in water transport, these results suggest that the faster component of water transport is channel-mediated whereas the slower component of water transport is lipid-mediated. Possible explanations for the functional heterogeneity in rat endosomes are discussed below.

TABLE I

Temperature Dependence of P_f in Rabbit Endosomes

Temperature	P_f	% Inhibition by $HgCl_2$
°C	*cm/s*	
15	0.0075 ± 0.001	67 ± 3
21	0.0091 ± 0.001	56 ± 4
28	0.011 ± 0.002	53 ± 6
35	0.015 ± 0.002	35 ± 5

Endosomes containing 100 mM mannitol and 5 mM K phosphate at pH 7.4 were subject to a 100-mM inward sucrose gradient. P_f values were calculated as described in Methods. Values represent the mean ± SD for measurements performed 10 times in three separate endosome preparations. The fitted activation energy from an Arrhenius plot was 6.4 ± 0.5 kcal/mol (r = 0.97). For inhibitor studies, 0.5 mM $HgCl_2$ was incubated with endosomes for 5 min before experiments.

Proton Transport

Mechanisms of proton transport across the endosome membrane were examined by making use of the pH dependence of fluorescein-dextran fluorescence. Direct titration experiments showed that fluorescein-dextran fluorescence is absent at low pH and increases with deprotonation (pK_a 6.3). The shape of the fluorescence vs. pH titration curve for fluorescein-dextran entrapped in endosomes was identical to that for the dye in free solution, and was fitted closely over the pH range 4.5–8 by the empiric cube equation $pH = 7.22\ F^3 - 13.81\ F^2 + 10.27\ F + 3.705$, where F is fluorescence normalized to unity at pH 7.4.

Proton ATPase activity was measured from the time course of endosome acidification in response to the addition of external ATP (Fig. 3). Because endosomes are "inside-out" membranes, there was inward proton transport in response to ATP hydrolysis at an external binding site. Experiments were performed with K-containing buffers and valinomycin to eliminate induced diffusion potentials due to electrogenic proton pumping. Upon addition of ATP there was a rapid drop in fluorescence followed by a plateau in which the rate of inward proton pumping became

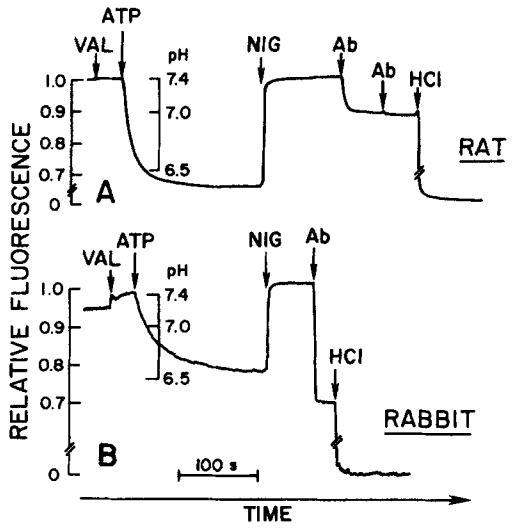

FIGURE 3. Measurement of proton ATPase activity in endosomes. Endosomes containing 100 mM KCl, 2 mM $MgCl_2$, and 5 mM K phosphate at pH 7.4 were voltage clamped with valinomycin as described in Methods. ATP was added to a final concentration of 5 mM. After acidification occurred, nigericin was added to collapse the pH gradient. This was followed by addition of the anti-fluorescein antibody to quench the signal from external fluorescein-dextran, followed by HCl to quench the signal from all fluorescein-dextran. Calculated rates of acidification and minimum pH values are given in the text.

equal to the rate of passive proton efflux. Upon addition of nigericin to dissipate the proton gradient, fluorescence promptly returned to its level prior to ATP addition. Upon addition of the anti-fluorescein antibody, there was a rapid drop in fluorescence due to quenching of external fluorescein-dextran. Complete quenching of external dye was demonstrated by the lack of effect of further antibody additions. HCl was added at the end of the experiment to quench the fluorescein-dextran fluorescence everywhere to give the baseline signal.

The scale showing absolute endosome pH was calculated from the fluorescence vs. pH calibration curve and the total intraendosome fluorescence determined from the signal remaining after antibody quenching. In three separate sets of experiments, the initial rate of pH drop after ATP addition was 0.17 ± 0.03 (rat) and 0.029 ± 0.005 pH unit/s (rabbit); the minimum endosome pH after steady state was achieved was 6.4 ± 0.1 (rat) and 6.5 ± 0.2 (rabbit). Addition of 0.5 mM NEM strongly inhibited endosome acidification after ATP addition; the initial rate of pH

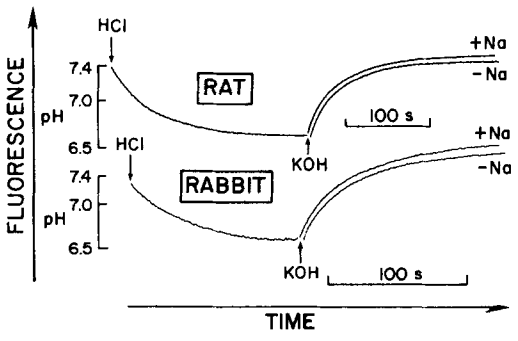

FIGURE 4. Passive and sodium-dependent proton transport in endosomes. Endosomes containing 100 mM KCl, 2 mM $MgCl_2$ and 5 mM K phosphate at pH 7.4, and voltage-clamped with valinomycin were stirred continuously. HCl (0.45 μmol) was added to drop external pH to 6.5. After endosome pH stabilized, KOH (0.45 μmol) was added to return pH to 7.4 in the presence of 20 mM NaCl (+Na) or of 20 mM choline Cl (−Na). Calculated rates of alkalinization are given in the text.

drop was 0.004 ± 0.001 (rat) and 0.006 ± 0.002 pH unit/s (rabbit) and the minimum endosome pH was 7.2 ± 0.1 (rat) and 7.3 ± 0.1 (rabbit). In separate experiments, 0.5 mM NEM did not alter passive proton permeability, indicating that the effect of NEM was a direct inhibition of the proton pump. The compounds oligomycin (10 μM) and vanadate (0.5 mM) did not alter ATP-dependent acidification significantly, indicating the presence of a "vacuolar-type" proton ATPase (Stone and Xie, 1988).

The presence of sodium-proton exchange in endosomes was examined from the effect of an inward sodium gradient on proton efflux (endosome alkalinization) (Fig. 4). Upon addition of HCl to drop external pH to 6.5, there was a time-dependent decrease in fluorescence corresponding to passive proton permeability. The rate of this decrease is similar to that reported in studies of passive proton permeability in proximal tubule apical vesicles (Verkman and Ives, 1986), however, comparison of proton permeability coefficients is not possible without knowledge of the internal endosome buffer capacity. Upon addition of KOH to return external pH to 7.4, there was a time-dependent increase in fluorescence (initial rate: 0.028 ± 0.001 [rat] and 0.036 ± 0.002 pH unit/s [rabbit] $n = 3$). The kinetics of this increase were not altered by 20 or 50 mM Na (20 mM, 0.029 ± 0.002 [rat] and 0.036 ± 0.001 pH unit/s [rabbit]; 50 mM, 0.027 ± 0.002 [rat] and 0.035 ± 0.002 pH unit/s [rabbit]). In contrast, in similar studies on apical vesicles from proximal tubule, there was a 5–10-fold stimulation of alkalinization in response to an inward sodium gradient (Warnock et al., 1982; Ives et al., 1986). The stimulation was inhibited by amiloride and was attributed to presence of sodium-proton exchange. In separate experiments, 20 and 50 mM NaCl was added to endosomes after the minimum pH was obtained in response to ATP addition. There was no measurable effect of sodium addition on endosome pH, which supports our conclusion that sodium/proton exchange, though present on the apical membrane, is absent in endosomes.

Nonelectrolyte Transport

The permeability of rabbit endosomes to a series of small polar nonelectrolytes was measured to compare with results reported in apical vesicles from rabbit renal cortex. Endosomes were subjected to an inward solute gradient in the stopped-flow apparatus (Fig. 5). There was a rapid drop in fluorescence due to osmotic water efflux from labeled endosomes, followed by a slower increase in fluorescence due to solute and water entry. Solute permeability coefficients in units of centimeters per second were calculated from the detailed time course of fluorescence increase by comparing data to theoretical curves calculated from the Kedem-Katchalsky equations (Chen et al., 1988).

The data in Fig. 5 show rapid influx of ethylene glycol and slower influx of glycerol and urea in endosomes. There was no measurable entry of sucrose over the 20 s shown, indicating that the fluorescence increase was due to specific solute influx rather than to nonspecific solute leak. In three sets of experiments, the calculated permeability coefficients in centimeters per second $\times 10^{-6}$ for a series of polar nonelectrolytes were 1.1 ± 0.2 (urea), 1.0 ± 0.1 (glycerol), and 14 ± 2 (ethylene glycol). Corresponding permeability coefficients reported in brush border vesicles were (centimeters per second $\times 10^{-6}$): 2.0 (urea), 1.1 (glycerol), and 19 (ethylene glycol)

(Verkman et al., 1985; Chen and Verkman, 1987). Endosome urea transport was not inhibited by 250 μM phloretin.

The presence of sodium-glucose cotransport in endosomes was examined from the time course of fluorescence in response to an inward glucose gradient in the presence of sodium and a potassium/valinomycin voltage clamp (see Methods). As shown in the bottom curve in Fig. 5, which is representative of two separate sets of experiments, there was no measurable entry of glucose over 20 s. In addition, there was no effect of 250 μM phloretin, a glucose transport inhibitor, on the curve shape (not shown). If sodium-glucose cotransport were present with activity similar to that in the proximal tubule apical membrane, it is predicted that the fluorescence should have increased to 50% of its final value within 30 s under the experimental conditions (Hopfer and Groseclose, 1980).

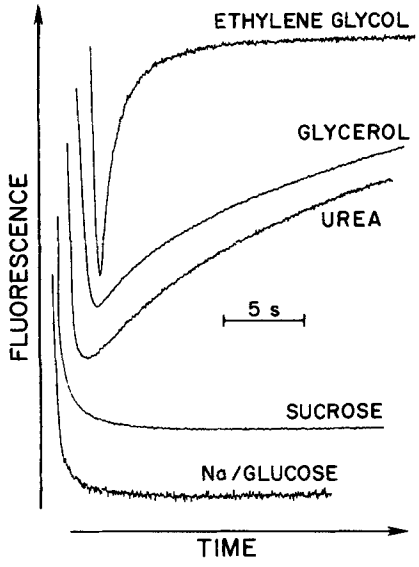

FIGURE 5. Nonelectrolyte and sodium-glucose cotransport in rabbit endosomes. (*Top four curves*) Endosomes containing 100 mM mannitol and 5 mM K phosphate at pH 7.4 were subject to a 100-mM inward osmotic gradient of each nonelectrolyte solute in the stopped-flow apparatus. Curves were offset and scaled for visual clarity. (*Bottom curve*) Endosomes in 25 mM NaCl, 25 mM KCl, and 5 mM K phosphate at pH 7.4 containing valinomycin were subject to a 100 mM D-glucose gradient.

Colocalization of Water Channels and Proton Pumps

The dual dependence of fluorescein-dextran fluorescence on endosome pH and volume was used to examine whether functional water channels and proton pumps colocalized in a single population of endosomes. If an endosome contained both a water channel and a proton pump, then ATP addition would result in endosome acidification, and a decrease in the signal amplitude of the fluorescence time course in response to an inward osmotic gradient. If water channels and proton pumps were present in separate endosome populations, then ATP addition would not alter the fluorescence time course of water transport in endosomes containing water channels because the pH of that population of endosomes would not decrease.

To interpret quantitatively the decrease in signal amplitude in osmotic water experiments in terms of a decrease in endosome pH resulting from proton pump activity, it was necessary to measure the pH dependence of fluorescein-dextran self-

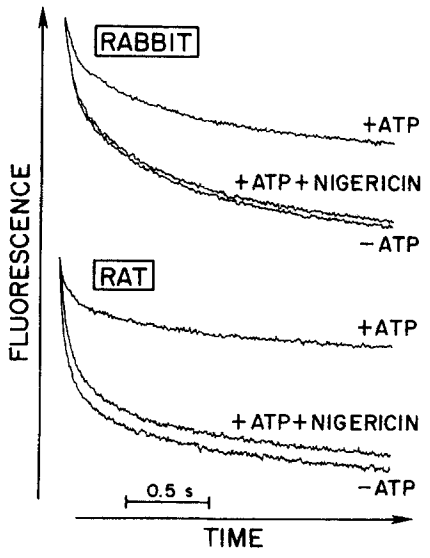

FIGURE 6. Colocalization of water channels and proton pumps in endosomes. Endosomes containing 100 mM KCl, 2 mM $MgCl_2$, and 5 mM K phosphate at pH 7.4 were subject to a 100-mM inward sucrose gradient in the stopped-flow apparatus. Curves were offset in the y direction to start at the same point. *+ATP* indicates addition of 5 mM ATP to endosomes 3–5 min before stopped-flow measurements. *+ATP +Nigericin* indicates addition of 5 μM nigericin to the endosome suspension containing ATP. Nigericin itself did not alter the fluorescence signal in the absence of ATP (not shown). Fitted results are summarized in the text and in Table II.

quenching in endosomes. Rabbit endosomes at pH 6.0, 6.5, 7.0, and 7.4 in 100 KCl and 5 mM phosphate were subjected to a 110-mM inward sucrose gradient in the absence of a pH gradient. Although pH did not alter fitted exponential time constants significantly, the relative amplitudes of the fluorescence signals were 1 (7.4), 0.86 ± 0.02 (7.0), 0.65 ± 0.03 (6.5), and 0.40 ± 0.02 (6.0). Because these amplitudes paralleled closely the pH vs. fluorescence titration of fluorescein-dextran, it follows that pH modifies the total fluorescence of fluorescein-dextran, but not the fractional decrease in fluorescence caused by a decrease in endosome volume.

ATP addition resulted in a marked decrease in signal amplitude in osmotic water transport experiments performed on endosomes from rat and rabbit (Fig. 6). There was no effect of ATP on measured osmotic water permeabilities. To show that this

TABLE II

Colocalization of Proton Pumps and Water Channels in Endosomes

	P_f	Relative amplitude
	$cm/s \times 10^{-3}$	
Rabbit (n = 9)		
−ATP (control)	9.2 ± 0.3	0.98 ± 0.04
+ATP	9.5 ± 0.4	0.57 ± 0.03
+ATP +nigericin	9.5 ± 0.3	1.00
Rat (n = 3)		
−ATP (control)	29 ± 4/2.3 ± 0.2	0.95 ± 0.06/0.99 ± 0.06
+ATP	24 ± 5/2.1 ± 0.4	0.52 ± 0.05/0.54 ± 0.03
+ATP +nigericin	26 ± 3/2.0 ± 0.2	1.00/1.00

Experiments were performed as described in the legend to Fig. 6 at 23°C. Data represent the mean ± SE of fitted single (rabbit) or double exponential curves (rat). Relative amplitudes were normalized to that for the +ATP +nigericin experiments.

decrease was not the result of a nonspecific optical effect, nigericin was added to collapse the ATP-induced pH gradient. Nigericin addition resulted in the return of the signal amplitude to the pre-ATP level. Results from a series of similar experiments are summarized in Table II. In rabbit endosomes, the decrease in signal amplitude from 1.00 to 0.57 with ATP addition corresponded closely to the decrease in the steady-state fluorescence signal upon addition of ATP to endosomes (0.55 ± 0.03) in proton ATPase experiments (see Fig. 3). These results indicate that the majority of endosomes containing water channels also contain proton pumps. Similarly, the decrease in signal amplitudes for each component of the double exponential fit in rat endosomes (0.52 and 0.54) corresponded closely to the decrease in steady-state fluorescence (0.50 ± 0.03) upon ATP addition. These data show that both populations of endosomes from rat proximal tubule contain proton pumps (see Discussion).

To investigate whether proton pumps were present in endosomes at the time of membrane retrieval, proton pump activity and the effect of ATP on the osmotic water time course were measured in endosomes isolated at 4 and 15 min after fluorescein-dextran infusion into rabbits. Paired comparisons in the same animal were made possible by removing one kidney at 4 min (with renal artery and vein ligation to prevent hemorrhage) and the second kidney at 15 min. In two sets of experiments, there was no significant difference between endosomes isolated at 4 and 15 min in proton ATPase activity (minimum pH: 6.5 ± 0.2, 4 min; 6.6 ± 0.1, 15 min) or in the effect of ATP on the osmotic water time course (signal amplitude of +ATP experiment normalized to amplitude of the +ATP +nigericin experiment: 0.56 ± 0.05, 4 min; 0.59 ± 0.03, 15 min). The total signal intensity of data obtained with the endosomes isolated at 4 min was less than threefold of that obtained with endosomes isolated at 15 min, which is as expected because of the difference in time during which labeled endosomes were produced. These results indicate that the water transport and proton pump characteristics of endosomes do not change during the 4–15 min time interval after endocytosis from the apical surface.

DISCUSSION

An in vivo labeling technique has been used to label endosomes from the proximal tubule apical membrane with a membrane-impermeant marker, fluorescein-dextran. The indicator was infused into living animals, entered renal tubular fluid by glomerular filtration, and was taken up into tubular cells by fluid-phase endocytosis. Morphological studies showed that virtually all endosomes isolated from the superficial renal cortex were derived from the apical membrane of proximal tubule cells. Once taken up into endosomes, the fluorescein-dextran remained entrapped during the brief homogenization and centrifugation procedures used for preparation of crude microsomes. Specific information about transport processes across the endosomal membrane was obtained using the crude microsomal preparation by making use of the dependence of fluorescein-dextran fluorescence on endosome volume and pH. This unique dual dependence was important for demonstration of the functional colocalization of water channels and the proton ATPase as discussed below.

Osmotic water transport was quantitated in endosomes from the time course of

fluorescence in response to an inward osmotic gradient. The dependence of entrapped fluorescein-dextran fluorescence on endosome volume was nearly linear as determined from the dependence of the amplitude of the kinetic signal on the magnitude of the inward osmotic gradient. Although the physicochemical basis for the dependence of fluorescence on volume has not been established, it is likely that both self-quenching effects and interactions between the fluorophore and proteins at the inner endosome membrane are important (Chen et al., 1988).

Water transport across endosomes from rabbit proximal tubule fitted well to a single, functionally homogeneous component, suggesting that the water transport properties and geometry of endosomes did not vary greatly. The high P_f, low E_a, and reversible inhibition of P_f by mercurials indicate that water transport across the endosome membrane occurs via a channel or pore mechanism (Finkelstein, 1987). The osmotic water permeability properties of the endosome membrane were quite similar to those reported in brush border membrane vesicles isolated from the apical membrane of proximal tubule and those in the apical membrane of the intact perfused proximal tubule. In rabbit endosomes, P_f was 0.009 cm/s (23°C), E_a was 6.4 kcal/mol, and P_f was inhibited reversibly with 1 mM $HgCl_2$ (74%) with a K_I of ~0.3 mM. In rabbit brush border vesicles, P_f was 0.007 cm/s (23°C), E_a was ~4 kcal/mol (15–35°C), and P_f was inhibited reversibly with 1 mM $HgCl_2$ (~50%) with a K_I of ~0.2 mM (Meyer and Verkman, 1987).

Interestingly, osmotic water transport in brush border vesicles from rat has been reported to be functionally heterogeneous, consisting of two distinct vesicle populations that have different water transport properties (Pratz et al., 1986; van Heeswijk and van Os, 1986). It was reported that P_f for the faster component of water transport was ~0.06 cm/s and inhibited by mercurials. In the present study, we also find two distinct rates of water transport in endosomes from rat renal cortex having very different P_f, E_a, and $HgCl_2$ inhibition. Therefore the two types of water transport cannot be accounted for by heterogeneity in endosome geometry. In addition, because the fluorescence time course was biexponential, the two distinct components of water transport cannot be present on the same endosome. These results are consistent with endocytosis of apical membrane patches from two proximal tubule cells types (e.g., early vs. late proximal tubule) having different apical membrane water permeabilities, or with endocytosis of two distinct apical membrane patches of differing composition from the same cell type.

Endosomes from both rat and rabbit proximal tubule contain a proton ATPase that is sensitive to NEM and insensitive to oligomycin and vanadate. These results are in agreement with previous reports of an endosomal proton ATPase identified by acridine orange methods in an "endosomal" fraction obtained by sucrose or Percoll gradient separation of homogenized renal cortex (Sabolic et al., 1985; Gurich and Warnock, 1986; Sabolic and Burckhardt, 1986). In these previous reports, results obtained using a fluorescein-dextran labeling technique were referred to briefly, however no primary data were given. In addition, it was not possible in those studies to quantitate the initial rate of or maximal endosomal acidification. The entrapment of a fluid-phase marker of endocytosis in the present study has the important advantage that uncertainties in the vesicle origin of the proton ATPase signal are eliminated (Ohkuma et al., 1982).

The presence of an Na/H exchanger in proximal tubule endosomes has been controversial. Using a Percoll gradient technique to purify endosomes, Sabolic et al. (1985) report the absence of an Na/H exchanger, whereas using a sucrose gradient technique, Gurich and Warnock (1986) report the presence of an amiloride-insensitive Na/H exchanger. Our results exclude the presence of an Na/H exchanger in endosomes from both rat and rabbit proximal tubule. Under the conditions of our experiment, there would have been a greater than fivefold stimulation of endosome alkalinization if an Na/H exchanger were present having similar activity to that in the proximal tubule apical membrane (Warnock et al., 1982; Ives et al., 1986); a less than 1.2-fold stimulation would have been detectable experimentally. It is not possible however to rule out the presence of inactivated Na/H exchangers in the endosomal membrane.

These findings demonstrate that endocytosis results in the selective internalization of membrane transporters. Both the Na/H exchanger and Na/glucose cotransporter, major transport proteins in the proximal tubule apical membrane, are absent (or at least inactivated) in endosomes. The endosomal water transporter appears to have similar activity to the water transporter characterized in apical membrane vesicles. Presence of a water channel in endosomes is clearly not a universal phenomenon; endosomes from rat renal papilla obtained in the absence of vasopressin pretreatment do not contain water channels (Verkman et al., 1988). A proton ATPase, thought to be active on the proximal tubule apical membrane and important for urinary acidification (Preisig et al., 1987), does appear on the endosomal membrane. In fact the "strength" of the proton ATPase, measured by the fractional decrease in endosome fluorescence in response to ATP addition, was the same for endosomes isolated 4 and 15 min after fluorescein-dextran infusion. This finding suggests that the proton ATPase was present in the endosome membrane at the time of membrane retrieval from the apical surface, rather than added subsequently by an intracellular fusion event. Again, the presence of a proton ATPase is not a general feature of endosomes; endosomes obtained from renal papilla do not contain measurable proton ATPase activity (Lencer et al., 1988).

Although the focus of the studies reported here has been in the characterization of transporters on apical endosomes from proximal tubule, the results suggest novel physiological regulatory mechanisms that are subjectable to experimental verification. Recent work from this laboratory has shown that steady-state transepithelial P_f in proximal convoluted tubule decreases as osmotic gradient size increases, suggesting that apical membrane water permeability may be regulated by water flow or osmotic gradient size (Berry and Verkman, 1988). In cortical collecting tubule, there is evidence that exocytic-endocytic cycling of subcellular membranes is controlled both hormonally and by transcellular volume flow (Kuwahara and Verkman, 1989). Vasopressin-induced endosomes from both kidney collecting tubule (Verkman et al., 1988) and toad urinary bladder (Shi and Verkman, 1989) have been shown to contain functional water channels. Our finding of the selective presence of water channels in endocytic vesicles from proximal tubule raises the possibility that transcellular water transport in proximal tubule may, under some circumstances, be regulated by exocytic and endocytic cycling. Recently developed fluorescence techniques for measurement of tubule water transport in real-time and for measure-

ment of tubule endocytosis (Kuwahara et al., 1988) should provide the methodology to examine this hypothesis.

The presence of an NEM-sensitive proton ATPase in endosomes also raises the possibility that proximal tubule acidification may in part be regulated, however, the relatively minor importance of an apical H ATPase under physiological conditions would minimize the consequences of a change in apical proton ATPase activity. Endocytic retrieval of sodium-proton exchangers could have a major effect on proximal tubule acidification, however, our results indicate the absence of sodium-proton exchange in endosomes. Finally, the biological significance of the interesting finding that endosomes contain both water channels and proton pumps is unclear at this time. The selective colocalization of water channels and proton pumps may simply be a consequence of the selective exclusion of other plasma membrane components from the endocytic process, or it may be important to provide an acidic environment for subsequent subcellular sorting and targeting of endocytic membrane components.

This work was supported by grants DK-35124, DK-39354, and HL-42368 from the National Institutes of Health, a grant-in-aid from the American Heart Association, and a grant from the National Cystic Fibrosis Foundation. Dr. Lencer was supported by NIH training grant AM-07477 and a grant from the Hood Foundation. Dr. Verkman is an established investigator of the American Heart Association.

Original version received 29 August 1988 and accepted version received 7 November 1988.

REFERENCES

Berry, C. A., and A. S. Verkman. 1988. Osmotic gradient dependence of osmotic water permeability in the rabbit proximal convoluted tubule. *Journal of Membrane Biology.* 105:33–43.

Bode, F., H. Pockrandt-Hemstedt, K. Bauman, and R. Kinne. 1974. Analysis of pinocytic vesicles from rat kidney cortex. *Journal of Cell Biology.* 63:998–1003.

Chen, P.-Y., D. Pearce, and A. S. Verkman. 1988. Membrane water and solute permeability determined quantitatively by self-quenching of an entrapped fluorophore. *Biochemistry.* 27:5713–5718.

Chen, P.-Y., and A. S. Verkman. 1987. Non-electrolyte transport across renal proximal tubule cell membranes measured by tracer efflux and light scattering. *Pflügers Archiv.* 408:491–496.

Finkelstein, A. 1987. Water movement through lipid bilayers, pores and plasma membranes: theory and reality. Distinguished Lecture Series of the Society of General Physiologists. Wiley-Interscience, New York. 153–201.

Fromter, E. 1984. Viewing the kidney through microelectrodes. *American Journal of Physiology.* 247:F695–F705.

Gurich, R. W., and D. G. Warnock. 1986. Electrically neutral Na^+-H^+ exchange in endosomes obtained from rabbit renal cortex. *American Journal of Physiology.* 251:F702–F709.

Hopfer, U., and R. Groseclose. 1980. The mechanism of Na^+-dependent D-glucose transport. *Journal of Biological Chemistry.* 255:4453–4462.

Ives, H. E., P.-Y. Chen, and A. S. Verkman. 1986. Renal brush border Cl/OH exchange is coupled exclusively by electric potential. *Biochimica et Biophysica Acta.* 863:91–100.

Kim, Y., N. P. Illsley, and A. S. Verkman. 1988. Rapid fluorescence assay of glucose and neutral volume transport using an entrapped volume indicator. *Analytical Biochemistry.* 172:403–409.

Kuwahara, M., C. A. Berry, and A. S. Verkman. 1988. Measurement of osmotic water transport in

perfused cortical collecting tubules by fluorescence microscopy. *Biophysical Journal.* 54:595–602.

Kuwahara, M., and A. S. Verkman. 1989. Transcellular water flow modulates water channel exocytosis and endocytosis in kidney collecting tubule. Kidney International. 35:188. (Abstr.)

Lencer, W. I., D. Brown, M. A. Arnaout, D. A. Ausiello, and A. S. Verkman. 1988. Endocytic vesicles from renal papilla which recycle the vasopressin-sensitive water channel do not contain an H^+ ATPase. *Journal of Cell Biology.* 107:810*a*. (Abstr.)

Macey, R. I. 1984. Transport of water and urea in red blood cells. *American Journal of Physiology.* 246:C195–C203.

Meyer, M. M., and A. S. Verkman. 1987. Evidence for water channels in proximal tubule cell membranes. *Journal of Membrane Biology.* 96:107–119.

Ohkuma, S., Y. Moriyama, and T. Takano. 1982. Identification and characterization of a proton pump on lysosomes by fluorescein isothiocyanate-dextran fluorescence. *Proceedings of the National Academy of Sciences.* 79:2758–2762.

O'Neil, R. G., and J. M. Reid. 1988. Cell swelling and a diacylglycerol analogue activate endocytosis in renal proximal straight tubule. *FASEB Journal Abstracts.* 2:A1284. (Abstr.)

Park, C. H. 1988. The role of cAMP and calcium in the regulation of endocytosis in the proximal tubule of the rabbit kidney. *FASEB Journal Abstracts.* 2:A494. (Abstr.)

Pratz, J., R. Ripoche, and B. Corman. 1986. Evidence for a proteic pathway for water transport in rat renal cortex. *Biochimica et Biophysica Acta.* 856:259–266.

Preisig, P. A., H. E. Ives, E. J. Cragoe, R. J. Alpern, and R. C. Rector. 1987. Role of the Na^+/H^+ antiporter in rat proximal tubule bicarbonate absorption. *Journal of Clinical Investigation.* 80:970–978.

Rodman, J. S., L. Seidman, and M. G. Farquhar. 1986. The membrane composition of coated pits, microvilli, endosomes, and lysosomes is distinctive in the rat kidney proximal tubule cell. *Journal of Cell Biology.* 102:77–87.

Sabolic, I., and G. Burckhardt. 1986. Characteristics of the proton pump in rat renal cortical endocytic vesicles. *American Journal of Physiology.* 250:F817–F826.

Sabolic, I., and G. Burckhardt. 1988. Proton ATPase in rat renal cortical endocytic vesicles. *Biochimica et Biophysica Acta.* 937:398–410.

Sabolic, I., W. Haase, and G. Burckhardt. 1985. ATP-dependent H^+ pump in membrane vesicles from rat kidney cortex. *American Journal of Physiology.* 248:F835–F844.

Shi, L.-B., and A. S. Verkman. 1989. Very high water permeability in vasopressin-dependent endocytic vesicles in toad urinary bladder. *Biophysical Journal.* 55:159*a*. (Abstr.)

Stone, D. K., and X.-S. Xie. 1988. Proton translocating ATPases: issues in structure and function. *Kidney International.* 33:767–774.

Strauss, W. 1964. Occurrence of phagosomes and phagolysosomes in different segments of the nephron in relation to reabsorption, transport, digestion and extrusion of intravenously injected horseradish peroxidase. *Journal of Cell Biology.* 21:295–308.

van Heeswijk, M. P. E., and C. H. van Os. 1986. Osmotic water permeabilities of brush border and basolateral membrane vesicles from rat renal cortex and small intestine. *Journal of Membrane Biology.* 92:183–193.

Verkman, A. S., J. A. Dix, and J. L. Seifter. 1985. Water and urea transport in renal microvillus membrane vesicles. *American Journal of Physiology.* 248:F650–F655.

Verkman, A. S., and H. E. Ives. 1986. Anomalous driving force for renal brush border H^+/OH^- transport characterized using 6-carboxyfluorescein. *Biochemistry.* 25:2876–2882.

Verkman, A. S., W. Lencer, D. Brown, and D. A. Ausiello. 1988. Endosomes from kidney collecting tubule contain the vasopressin-sensitive water channel. *Nature.* 333:268–269.

Wade, J. B., K. L. Stetson, and S. A. Lewis. 1981. ADH action: evidence for a membrane shuttle hypothesis. *Annals of the New York Academy of Sciences.* 372:106–117.

Warnock, D. G., W. W. Reenstra, and V. J. Yee. 1982. Na/H antiporter of brush border vesicles: studies with acridine orange uptake. *American Journal of Physiology.* 242:F733–F739.

Weyer, P., W. I. Lencer, A. S. Verkman, D. A. Ausiello, and D. Brown. 1988. Correlation of endosome morphology and function using a single probe, FITC-dextran. *Journal of Cell Biology.* 107:111*a*. (Abstr.)

Whittembury, G., A. Paz-Aliaga, A. Biondi, P. Carpi-Medina, E. Gonzalez, and H. Linares. 1985. Pathways for volume flow and volume regulation in leaky epithelia. *Pflügers Archiv.* 405 (Suppl. 1):S17–S22.